



UNIVERSIDADE DO SUL DE SANTA CATARINA
PROGRAMA DE PÓS-GRADUAÇÃO EM CIÊNCIAS AMBIENTAIS

THIAGO DE ALCÂNTARA BRAGLIA

**ESPUMAS RÍGIDAS DE POLIURETANO MODIFICADAS COM
CIMENTO LODO ANODIZADO DE ALUMÍNIO E LODO DE VIDRO**



Palhoça, 2019

THIAGO DE ALÂCANTARA BRAGLIA

**ESPUMAS RÍGIDAS DE POLIURETANO MODIFICADAS COM
CIMENTO LODO ANODIZADO DE ALUMÍNIO E LODO DE VIDRO**

Dissertação apresentada ao Programa de Pós-Graduação em Ciências Ambientais, como quesito parcial à obtenção do título de Mestre em Ciências Ambientais

Orientador: Dra. Rachel Faverzani Magnago

Palhoça 2019

B79	<p>Braglia, Thiago de Alcântara, 1989- Espumas rígidas de poliuretano modificadas com cimento lodo anodizado de alumínio e lodo de vidro / Thiago de Alcântara Braglia. – 2019. 48 f. : il. color.; 30 cm</p> <p>Dissertação (Mestrado) – Universidade do Sul de Santa Catarina, Pós-graduação em Ciências Ambientais. Orientação: Prof. Dr. Rachel Faverzani Magnago</p> <p>1. Resistência de materiais. 2. Poliuretanas. 3.Cimento. I. Magnago, Rachel Faverzani. II. Universidade do Sul de Santa Catarina. III. Título.</p> <p>CDD (21. ed.) 620.112</p>
-----	--

Ficha catalográfica elaborada por Carolini da Rocha CRB 14/1215



UNISUL
**PROGRAMA DE PÓS-GRADUAÇÃO EM CIÊNCIAS AMBIENTAIS –
MESTRADO**

ATA N°06/2019 DE DEFESA PÚBLICA DE DISSERTAÇÃO

Aos dez dias do mês de julho de dois mil e dezenove às catorze horas, na sala 116 – Bloco D, na Unidade Universitária Pedra Branca da Universidade do Sul de Santa Catarina, foi realizada a sessão pública de apresentação e defesa de Dissertação de Mestrado de **Thiago de Alcântara Braglia**, como requisito para obtenção do título de Mestre em Ciências Ambientais, de acordo com o Regimento Interno do Programa de Pós-Graduação em Ciências Ambientais - PPGCA. A comissão avaliadora foi composta pelos seguintes professores: - Dra. Rachel Faverzani Magnago, orientadora e presidente da banca; - Dr. Américo Cruz Júnior, avaliador externo da Universidade Federal de Santa Catarina (UFSC); - Dra. Lisiane Ilha Librelotto, avaliadora externa da Universidade Federal de Santa Catarina (UFSC); - Dra. Paola Egert Ortiz, avaliadora interna da Universidade do Sul de Santa Catarina (UNISUL). A dissertação tem como título: **"ESPUMAS RÍGIDAS DE POLIURETANO MODIFICADAS COM CIMENTO LODO DE ALUMÍNIO ANODIZADO E LODO DE VIDRO"**. Área de concentração: Tecnologia, Ambiente e Sociedade e linha de pesquisa: Tecnologia & Sociedade. Após a apresentação, o mestrando foi arguido pelos professores da banca. Feitos os questionamentos e ouvidas as explicações, a banca avaliadora emitiu o seguinte parecer:

Aprovado

Aprovado condicionado

Reprovado

Obs: *considerar colocações de banca*

Nada mais havendo a tratar, foram encerrados os trabalhos e, após lida, foi a presente ata assinada pelo Mestrando e pelos membros da Comissão Avaliadora.

Dra. Rachel Faverzani Magnago: *Rachel Magnago*.

Dr. Américo Cruz Júnior: *Américo Cruz*.

Dra. Lisiane Ilha Librelotto: *Lisiane Ilha Librelotto*.

Dra. Paola Egert Ortiz: *Paola Ortiz*.

Discente Thiago de Alcântara Braglia: *Thiago Braglia*.

AGRADECIMENTOS

Em primeiro lugar quero agradecer a Deus, que sempre esteve presente, sempre cuidou e nunca desistiu de mim, por tantas aventuras ao redor mundo, tantos perrengues e situações em que tudo que tinha era eu e Você, sempre pude provar e viver da sua fidelidade, amor e carinho, muito obrigado Deus, meu melhor amigo.

Aos meus pais que sempre me apoiaram e mesmo quando saiu o resultado em que eu não estava na lista dos que receberiam a bolsa olharam nos meus olhos e falaram: Vá, faça a matrícula, tudo dará certo, nós te amamos e queremos o seu bem. Obrigado por não me deixarem desistir do mestrado. Hoje essa realidade pertence a vocês também, obrigado pela educação, pelo sustento, por tudo que vocês fizeram e fazem por mim, eu vejo amor em vocês, um amor não só a mim mas a todos de uma maneira exponencial e sem esperar nada em troca, admiro quem vocês são, exemplos para mim.

Ao meu irmão Israel e minha cunhada Franciane que a quase 4 anos atrás me deram algo que nunca poderia imaginar, me fizeram experimentar de sentimentos antes desconhecidos para mim, quando o João nasceu eu descobri outra forma de amor, outra forma de cuidado e carinho. Muito obrigado por quem vocês são, admiro a família que vocês constituíram e sou muito feliz em saber que faço parte dessa família agora bem maior (com as gêmeas), amo vocês.

A minha linda, compreensiva, paciente, meiga e querida namorada Aymeé, você é como um porto seguro em meio as aguas revoltas da minha vida, admiro a sua forma de pensar, de agir e de me entender mesmo quando eu não me entendo, te amo e oro para que o nosso futuro seja, na vontade de Deus, em amor e felicidade.

Ao meu amigo Matheus que mesmo com tantos conflitos sempre esteve presente, sempre me ajudou, inclusive nesse mestrado, fazendo os desenhos de CAD, os ensaios acústicos em pleno sol de verão, ao invés de estar na praia estava comigo dentro de um laboratório passando calor só porque eu precisava de ajuda, quero te dizer que te amo, que me considero um irmão mais velho seu, que me importo e quero a sua felicidade.

Tenho o coração muito grato a Deus por ter permitido que a minha orientadora fosse a melhor das melhores, mesmo sem nos conhecermos, você Rachel me aceitou, me ensinou, me empurrou, me corrigiu e fez com que o mestrado virasse uma realidade, obrigado pelo seu carinho mesmo sendo bem grossa as vezes (kkkk), você é muito excelente em tudo que faz,

cheia de alunos e pesquisas, sempre conseguindo dar atenção para cada um como se fossemos únicos, fazendo cada um crescer, transformando-nos em futuros profissionais, admiro sua forma de administrar as pessoas, de conciliar sua profissão com a vida familiar. Você se tornou um exemplo pra mim, muito obrigado, essa conquista é mais sua do que minha, obrigado por me ajudar.

A professora Paola, desde de o meu primeiro dia na graduação em engenharia ao dia de hoje, onde estou me tornando mestre vocês esteve presente, lembro-me bem quando tentamos os mestrado em engenharia de materiais e quando eu estava morando em Jerusalém e você veio me perguntar sobre tentar novamente um mestrado, muito obrigado por todos esses 9 anos de convivência, de me empurrar para a ciência, pelos estágios no laboratório de física, pelos anos na pesquisa do plasma, por fazer dar certo toda a parte física da minha pesquisa do mestrado. Você esteve presente na minha graduação, no meu mestrado, e quem sabe também estará em um doutorado, obrigado por ser quem você é, te admiro em sua seriedade em tudo que se propõem a fazer, muito obrigado.

A toda a equipe do LAQUE, e em especial ao Bruno que sempre esteve disposto a fazer a pesquisa, não importando se era pela manhã, a noite, sábados, férias ou feriados, você fez muito além do que era o necessário, que você continue sendo assim, alguém disposto a ajudar as pessoas, e claro se possível falando um pouco menos, as vezes até atordoava (kkkk), mas sou grato por todo o seu esforço. Agradeço também a Ana que possibilitou com que os testes de queima fossem realizados, pelo seu empenho e organização que possibilitou agora ao final da pesquisa a conferencia de todos os dados de uma forma muito organizada, e claro, pelos tantos cafés regados da sua porção diária de mal humor que quase sempre se tornava em sorrisos ao final do dia, que você possa continuar sendo essa pessoa que todos gostam de estar por perto, muito obrigado.

Agradeço a professora Heloisa que comprou a ideia dessa loucura que foi a minha pesquisa e conseguiu fazer com que a caixa acústica virasse uma realidade, pelo seu empenho em buscar nos alunos da engenharia civil a possibilidade de construção, fazendo com que a ciência se multiplicasse em conhecimentos entre graduação e mestrado, pelas analises do Lodo de Vidro e por sempre estar feliz e vibrante, quando abro a porta do laboratório sempre vejo o seu sorriso e a sua frase “oi querido, tudo certinho?”, sempre abraçando seus alunos como uma mãe, cuidando de cada um e forçando-os a melhorarem, você é muito especial.

Ao Marcos que usou de todo o seu conhecimento da engenharia elétrica para construir um dispositivo que conseguisse realizar as medições do teste térmico, por ter que se debruçar em conseguir resolver todos os problemas que aconteceram no percurso do projeto, por quase por fogo no laboratório por conta da corrente elétrica (kkkk), agradeço pela sua disposição, demanda de tempo e tratamento dos dados, o que falar da sua organização quanto as planilhas do excel? Parabéns, sei que serás um ótimo profissional.

Ao professor Cremona, comprehendo que não fui o seu melhor aluno de estatística e que muitas vezes eu não conseguia entender a logica que você tentava me ensinar para que fosse possível tratar os meus dados, mas quero te dizer que reconheço o quão excelente profissional o senhor é, vejo a excelência no que você se propõem a fazer, e sempre realizando a cima do proposto, muito obrigado professor, essa pesquisa também é sua conquista, “Muchas gracias”.

E por fim, mas não menos importante, agradeço a toda equipe do PPGCA, e dizer que sinto orgulho em fazer parte do inicio dessa historia, em especial agradeço a Marci que além de ser a alma do nosso programa nos mostrou e ensinou o quão forte podemos ser e que o nosso mundo não pode cair quando as circunstâncias ruins aparecem, você venceu não só o câncer mas venceu como pessoa, como mãe, como amiga, como profissional, você é muito mais forte do que aparenta, sua perseverança e luta são exemplos para mim, muito obrigado.

RESUMO

Este artigo tem como objetivo estudar a resistência físico-mecânica e ao fogo de compósitos de poliuretano/cimento (PuCem) contendo nanopartículas de lodos de vidro (GLA) e da anodização de alumínio (AAS). Os resultados de MEV mostram que a substituição de 24,5% do cimento por areia (SAN), AAS ou GLA, manteve a estrutura de alvéolos nos compósitos, incluída as análises de EDS e FTIR observa-se que a reação de hidratação do cimento forma aluminatos e silicatos hidratados. Através dos testes ANOVA-Tukey para as áreas e circularidades dos alvéolos tem-se que as áreas dos compósitos PuCemAas são significativamente diferentes aos PuCemGla e PuCemSan, sendo os dois últimos semelhantes entre si. Quanto a circularidade os compósitos PuCemGla e PuCemSan são significativamente diferentes aos PuCem e PuCemAas, novamente semelhantes entre si. A resistência à compressão diminuiu com a substituição do cimento pelos agregados. Os termogramas DTA/TGA foram semelhantes para os quatro compósitos e a matriz de PU. Os espécimes foram classificados como inflamáveis na posição horizontal, mas desclassificados na posição vertical (UL94). Os compósitos ofereceram uma barreira sonora entre 125 Hz e 8 kHz examinados. O ensaio do fio quente exibiu maior isolamento térmico para PuCemGla e PuCemAas. Conclui-se com gráfico radar que PuCemAas apresentou melhor resultado entre os compósitos preparados.

Palavras-chave:

Compósitos termo acústicas; Inflamabilidade; Lodo de anodização de alumínio; Lodo da lapidação de vidro.

ABSTRACT

This article aims to study the physico-mechanical strength and fire resistance of polyurethane/cement (PuCem) composites containing glass sludge nanoparticles (GLA) and nanoparticles from aluminium anodization (AAS). Scanning electron microscopy (SEM) results show that the replacement of 24.5% of the cement with sand (SAN), AAS or GLA maintained the alveolar structure in the composites; in addition, energy-dispersive X-ray spectroscopy (EDS) and Fourier transform infrared spectroscopy (FTIR) analyses show that the cement hydration reaction forms hydrated aluminates and silicates. Through the ANOVA-Tukey tests for the areas and circularity of the alveoli, the areas of the PuCemAas composites are significantly different from those of PuCemGla and PuCemSan, which are similar to each other. In their circularity, the PuCemGla and PuCemSan composites are significantly different from PuCem and PuCemAas, which are similar to each other. The compressive strength decreased upon replacing cement with the aggregates. The DTA/TGA thermograms were similar for the four composites and the polyurethane (PU) matrix. The specimens were classified as flammable in the horizontal position but declassified in the vertical position (UL94). The composites offered a sound barrier between 125 Hz and 8 kHz. The hot wire test showed higher thermal insulation for PuCemGla and PuCemAas. It is concluded from a radar chart that PuCemAas presented the best result among the prepared composites.

Keywords:

Thermoacoustic composites; Flammability; Aluminium-anodising sludge; Sludge from glass cutting and polishing.

SUMÁRIO

RESUMO.....	7
ABSTRACT.....	8
1. INTRODUÇÃO	10
2. CAPÍTULO	12
3. CONCLUSÃO.....	47

INTRODUÇÃO

A busca por desenvolvimento de produtos sustentáveis, que otimizem processos produtivos e redução de impactos socioambientais são de grande importância para a sociedade. A construção civil e todos processos e produtos são considerados um dos maiores geradores de resíduos no mundo. Desse modo, a utilização desses resíduos como matéria prima em outros processos produtivos são as tendências para que novos produtos sejam confeccionados, contemplando parte do propósito do plano de desenvolvimento sustentável da Organização das Nações Unidas. Placas termo acústicas a partir de poliuretano são amplamente utilizadas em diversas áreas da construção civil, porém são altamente inflamáveis e com altos índices de toxicidade da fumaça. A pesquisa realizada consistiu em produzir placas utilizando resíduos provenientes da construção civil obtendo resistência a inflamabilidade e barreira termo acústica, assim os compósitos para a obtenção de tais placas consistiram na reação de policondensação entre tolueno-2,6-diisocianato e polipropilenoglicol com adição de cimento, areias, lodo de anodização alumínio ou lodo de lapidação do vidro.

O trabalho teve como objetivo estudar a resistência físico-mecânica e ao fogo de compósitos de poliuretano/cimento (PuCem) contendo nanopartículas de lodos de vidro (GLA) e da anodização de alumínio (AAS). Os resultados de MEV mostram que a substituição de 24,5% do cimento por areia, AAS ou GLA, manteve a estrutura de alvéolos nos compósitos, incluída as análises de EDS e FTIR observa-se que a reação de hidratação do cimento forma aluminatos e silicatos hidratados. Através dos testes ANOVA-Tukey para as áreas e circularidades dos alvéolos tem-se que as áreas dos compósitos PuCemAas são significativamente diferentes aos PuCemGla e PuCemSan, sendo os dois últimos semelhantes entre si. Quanto a circularidade os compósitos PuCemGla e PuCemSan são significativamente diferentes aos PuCem e PuCemAas, novamente semelhantes entre si. A resistência à compressão diminui com a substituição do cimento, PuCem 0,7963 MPa para 0,2663 MPa, 0,2658 MPa e 0,1865 MPa, com areia, GLA e AAS, respectivamente. Os termogramas

DTA/TGA dos compósitos foram semelhantes com dois patamares endotérmica de perda de massa atribuídas a decomposição da matriz de PU, foram classificados como inflamáveis na posição horizontal, mas desclassificados para posição vertical (UL94). Os compósitos ofereceram uma barreira sonora para os oito comprimentos de ondas sonoras entre 125 Hz e 8 kHz. Os resultados do ensaio do fio quente demonstraram que os compósitos a partir dos resíduos proporcionaram maior isolamento térmico quando comparados com PuCem e PuCemSan. Pode-se concluir por análise de gráfico radar, onde as variáveis foram inflamabilidade vertical, inflamabilidade horizontal, compressão mecânica, teste acústico e térmico que PuCemAas apresenta melhor resultado, pois atingiu pontuação máxima em 3 dos 5 itens analisados, sendo estes inflamabilidade vertical e horizontal, e teste de resistência mecânica.

CAPÍTULO

Rigid polyurethane foam modified with cement, aluminium-anodising sludge and glass sludge

Abstract

This article aims to study the physico-mechanical strength and fire resistance of polyurethane/cement (PuCem) composites containing glass sludge nanoparticles (GLA) and nanoparticles from aluminium anodization (AAS). Scanning electron microscopy (SEM) results show that the replacement of 24.5% of the cement with sand (SAN), AAS or GLA maintained the alveolar structure in the composites; in addition, energy-dispersive X-ray spectroscopy (EDS) and Fourier transform infrared spectroscopy (FTIR) analyses show that the cement hydration reaction forms hydrated aluminates and silicates. Through the ANOVA-Tukey tests for the areas and circularity of the alveoli, the areas of the PuCemAas composites are significantly different from those of PuCemGla and PuCemSan, which are similar to each other. In their circularity, the PuCemGla and PuCemSan composites are significantly different from PuCem and PuCemAas, which are similar to each other. The compressive strength decreased upon replacing cement with the aggregates. The DTA/TGA thermograms were similar for the four composites and the polyurethane (PU) matrix. The specimens were classified as flammable in the horizontal position but declassified in the vertical position (UL94). The composites offered a sound barrier between 125 Hz and 8 kHz. The hot wire test showed higher thermal insulation for PuCemGla and PuCemAas. It is concluded from a radar chart that PuCemAas presented the best result among the prepared composites.

Keywords:

Thermoacoustic composites; Flammability; Aluminium-anodising sludge; Sludge from glass cutting and polishing.

1. Introduction

Environmental preservation is a globally discussed theme, and the urgent need to limit the use of natural resources has been highlighted. The interest of society in new ways of using waste by adding value and providing it with a longer life cycle contributes to sustainable development, in addition to generating opportunities for new businesses, employment and social inclusion [1, 2, 3].

The construction industry is a productive segment of the economy that can incorporate significant amounts of waste from other segments into product life cycles within its formulations; in this way, it becomes more sustainable and contributes to resolving environmental issues [4, 5].

Our research group performed studies on new materials for civil construction reusing waste from other production sectors, including polyethylene terephthalate [6, 7], ethylene vinyl acetate [8, 9], polyvinyl chloride [10] and polyurethane [11] residues. Furthermore, light aggregates (expanded clay, perlite and vermiculite) and fibres (cellulose and polypropylene) [12] and limestone-lime and clay-hemp aggregates [13] can be used to improve the thermal and acoustic properties of lime-cement mortars. A review of PU and its use in structural and infrastructural applications [14], as well as a study of the physico-mechanical characterization, microstructure and fire resistance of cement pastes containing Al_2O_3 nanoparticles, shows that even small amounts of nanoparticles (1%) can influence the properties of the material [15].

Despite these findings, no study has evaluated the replacement of cement with sand, glass sludge and aluminium-anodising sludge in polyurethane (PU) composites with respect to the

chemical stability and mechanical and thermoacoustic performance; the studied materials are used to make boards for wall revetments and masonry ceilings.

Noise pollution causes direct problems such as hearing loss and indirect problems such as irritability, stress, a lack of attention and low productivity. It can also cause psychological damage to homeowners whose residences have poor acoustic performance [16, 17, 18, 19].

Due to the high sound emission intensity generated by large cities, the demand for products with insulating characteristics and that can minimize sound in addition to providing thermal comfort has become greater. These products, for the most part, are manufactured using flammable and highly toxic chemical compounds [20]. The need to study materials that are safe to society and to the environment and that do not lose their acoustic isolation characteristics is of the utmost importance to fit the premise of sustainable development within the production processes [21, 22].

Studies on thermal insulation are based mainly on the increase in the cost of energy in both the production and conservation of thermally comfortable environments. The energy consumption in buildings for heating and cooling is responsible for approximately 40% of the global energy demand and approximately 60% of the total energy consumed in buildings [1, 16, 23]. This energy consumption highlights the importance of acoustic isolation because the noise levels should be compatible with the acoustic comfort of the surroundings. The materials for these applications must have characteristics of resistance to stress and deformability, dimensional stability, exclusion of water and vapor, fire resistance and durability [24, 25].

Despite PU's efficiency for thermal and acoustic insulation, its combustibility problem has become an urgent issue, and research has been widely performed on the development of safe materials [26, 27].

The recycling and use of waste to compete in the market is a welcome alternative. Large amounts of waste can be successfully applied in the fabrication of construction materials, thus improving their properties and durability [1, 6, 7, 21, 28]. The objective of this study was to investigate the properties of composites of PU/cement, sand, and aluminium-anodising or glass-cutting and polishing sludge as thermal and acoustic insulation; the current materials used in the civil construction industry are flammable.

2. Materials and methods

The aluminium-anodising sludge (AAS; HYDRA, Tubarão/SC-Brazil) and glass-cutting and polishing sludge (GLA; PERSONAL GLASS, Palhoça/SC-Brazil) were washed and filtered using a Buchner funnel, dried at 70 °C in an oven for 24 h and sieved through stainless steel sieves with a mesh size of 45 $\square\text{m}$.

The compositions of AAS and GLA were characterized by X-ray fluorescence and atomic absorption spectrometry assays. Table 1 shows the results of the atomic absorption spectrometry of AAS and GLA.

Table 1

Atomic absorption spectrometry results of aluminium-anodising sludge (AAS) and glass-cutting and polishing sludge (GLA).

Substance	AAS content (%)	GLA content (%)
Al ₂ O ₃	66.16	3.38
CaO	0.29	8.10
Fe ₂ O ₃	0.24	0.31
Na ₂ O	1.32	12.28
SiO ₂	0.48	64.75

P ₂ O ₅	0.24	-
K ₂ O	-	0.07
MgO	-	3.14
Loss on ignition	26.74	7.64

Table 1 shows 66% aluminium oxide in the AAS; thus, the element Al was predominant in the composition. X-ray diffractometry showed that the phases present in the AAS were aluminium hydroxide oxide [AlO(OH)], aluminium phosphate [AlPO₄] and aluminium hydroxide [Al(OH)₃].

In the GLA, atomic absorption spectroscopy showed 64% silicon oxide (predominance of the element silicon), and X-ray fluorescence showed that the phases were calcium silicate [CaSi₂O₅], sodium metasilicate [Na₂SiO₃], silicon oxide/coesite [SiO₂], silicon oxide/cristobalite [SiO₂] (Table 1).

The sand (GUAREZI, São Jose/SC-Brazil) was sieved through a stainless steel sieve with a mesh opening of 150 µm.

2.1 Composites

The composites were prepared by incorporating the cement (CPV-ARI Itambé, Balsa Nova/PR-Brazil), sand, and AAS or GLA in the polycondensation reaction between polypropylene glycol and toluene-2,6-diisocyanate (Arinos, São Paulo/SP, Brazil) [6]. The reagents were used as received and following safety standards; the polyol and isocyanate in their formulations are mainly provided by polypropylene glycol and toluene-2,6-diisocyanate. The raw materials (Table 2) were mixed and poured into a solid silicone mould (Fig. 1,

29.5x29.5x2.1 cm and a volume of 1053.4 cm³). The specimens were demoulded after 1 h; silicone was sprayed to facilitate the demoulding. The boards were cured for 21 days, the first 7 days submerged in water [21, 22].

Table 2

Amounts of reagents used to prepare composites of PuCem, PuCemSan, PuCemAas and PuCemGla.

Specimen	Polypropylene glycol (g)	Toluene-2,6-diisocyanate (g)	Cement (g)	Sand (g)	AAS (g)	GLA (g)
PuCem	54.1	81.3	81.3	-	-	-
PuCemAas	54.1	81.3	51.2	-	30.1	-
PuCemSan	54.1	81.3	51.2	30.1	-	-
PuCemGla	54.1	81.3	51.2	-	-	30.1

The composite boards were made with a square base (top view) with pyramidal shapes from their four side views (Table 2 and Fig. 1).

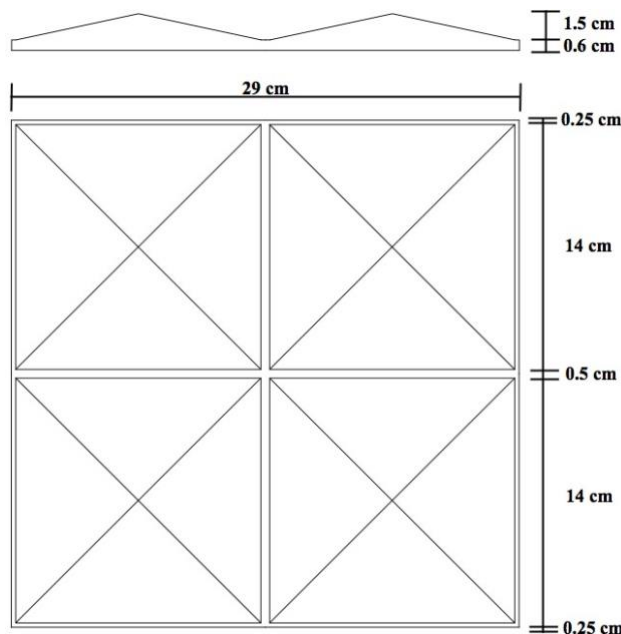


Figure 1. Mechanical design of the thermo-acoustic board mould.

The composites were produced in the different moulds according to the test requirements, maintaining the proportions shown in Table 2.

2.2 Scanning electron microscopy, morphological image analysis and chemical composition

The morphologies of the composites PuCem, PuCemSan, PuCemAas and PuCemGla were characterized by SEM (JEOL JSM-6390LV) with a voltage of 10 kV. The samples were fractured in liquid nitrogen and coated with gold.

FIJI/ImageJ software (<https://imagej.net/ImageJ> and <https://imagej.nih.gov/>) was used to process the SEM images, and the statistical analysis was performed with the XLStatistics - Excel Workbooks for Statistical Analysis (<http://www.deakin.edu.au/~rodneyc/XLStatistics>) application for MS Excel (2016). The protocol was systematized into five steps: dimensioning and cutting, look improvement, supervised classification, morphological analysis, and statistical analysis of morphometric data [29].

The scaling, i.e., pixel to real-size relationship, was performed with the help of the graphical scale bar stamped on the SEM image, and the data stamp was cut for the radiometric analysis. Radiometric improvements were made in the contrast, brightness and noise, as well as the elimination of outliers and equalization of the image frequency histogram. Filters were used in the frequency and spatial domains [30] to eliminate image noise; the filters used were the non-depigmented mask, despeckle, outlier (bright and dark), and median filters [31].

The classification sought patterns and homogeneous areas in the image, and the unknown pixels were compared and then statistically classified [32]. The ImageJ/FIJI Segmentation Trainable Weka plugin was used in this step, and the Gaussian Blur, Gaussian Difference and Entropy filters were used in this process. Thus, the polygons of the three classes analysed, i.e., the classes of shallow alveoli, deep/perforated alveoli and edges, were defined. Then, the resulting classes were used to generate probability maps and perform classification and segmentation based on the joint probability of each class.

The classified image was filtered to eliminate small areas of noise where one class overlapped the other. Then, the image was transformed into an 8-bit spectral image, in which a threshold process was applied to create 2-bit images (red, green and lilac) of each of the classes used in the study. Superficial cutting edges (class 1), shallow alveoli (class 2) and deep and perforated alveoli (class 3) were classified [20].

Finally, the morphometric parameters were calculated with these images to statistically evaluate the visualized forms of the material surface. This step was performed through the FIJI routine "Analyse" to demonstrate the morphometry of each of the classes (1, 2 and 3) of the images. The variables that were analysed and calculated by the computational model were the area (μm^2) and circularity ($4\pi * \text{area}/\text{perimeter}^2$). For the circularity, the value of 1.0 indicates a perfect circle, and a value that approaches 0.0 indicates an elliptical shape.

The results of this process generated plots of confidence intervals (CI) of 0.95 of the population mean of the variables for classes 1, 2 and 3 [33, 34]. ANOVA and Tukey's tests were also performed to determine the numerical and graphical relationships between the different composites.

In all ANOVA tests, the null hypothesis was that "all means are equal", and the alternative hypothesis was "not all means are equal"; the level of significance adopted was 0.05, and the test, according to the alternative hypothesis used, was a two-tailed test in which the equality of variances was assumed. These were performed for the alveoli (classes 2 and 3), and the means of the areas and the circularities for the composites were determined.

The chemical composition of the composites was analysed by infrared spectroscopy with a Fourier transform (FTIR) and energy-dispersive X-ray spectroscopy (EDS). The FTIR spectra were collected in the range of 4000 to 650 cm⁻¹ using a Perkin-Elmer apparatus (model 781).

2.3 Mechanical compressive strength

Tests of the compressive strength were performed on an EMIC model DL 30000 with a load cell of 5 kN at 25 °C. Eight specimens (5x5x4 cm) were subjected to pressure increments at a rate of 2 mm/s until a plastic deformation of 10% was attained; the force was applied perpendicularly to the direction of the foam growth [35].

2.4 Thermal stability and flammability

The thermogravimetric testing of the specimens was performed in a nitrogen atmosphere at a heating rate of 10 °C /min and temperature between 20 °C and 900 °C using a TGA Q5000 instrument (TA Instruments).

The flammability tests followed the standard practice for plastics conditioning for tests [36, 37]. According to the horizontal combustion flammability test [37, 38], a classification was only given when the combustion rate was lower than 38 mm/min; in the other cases, the specimens were declassified. Following the vertical combustion test, the classification criteria applied were V-0, V-1 and V-2 [7, 37, 39].

2.5 Acoustic Testing

With the use of a reverberating chamber (Fig. 2), tests were performed using a sound source positioned 90 cm from the wall in the emitting room and a decibel metre positioned 90 cm from the wall in the receiving room, measuring the sound intensity level in octave bands delimited between 0 Hz and 16000 Hz.

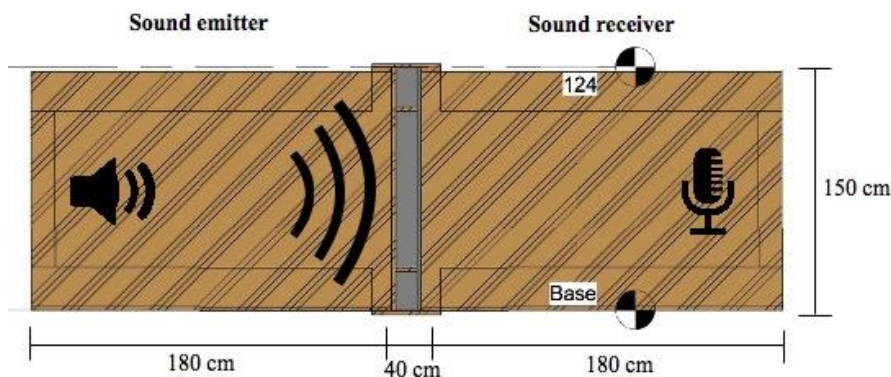


Figure 2. Schematics of the reverberating chamber.

The reverberating chamber has an internal wall that separates the receiving room (containing the detector of the sound intensity level) and the emitting room (Fig. 2 and Fig. 3). The sample holder is used as a room separator.

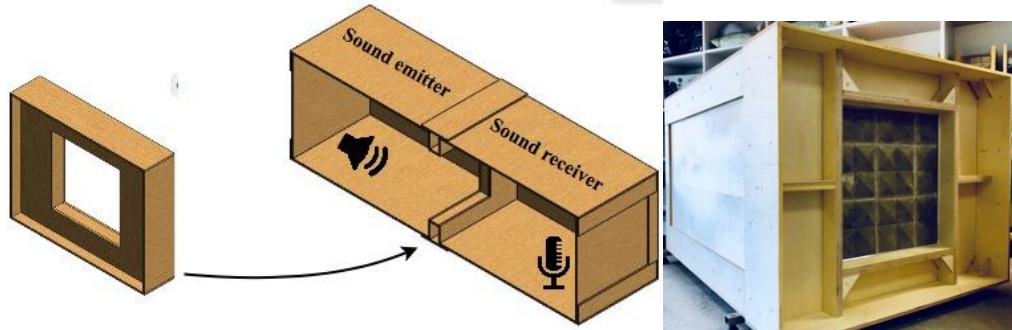


Figure 3. Sample holder of the reverberating chamber.

Fig. 3 shows an opening in the centre with dimensions of 80 cm x 80 cm. The sound intensity level was measured in the receiving room without and with a sample in the opening.

2.6 Heat capacity by hot wire method

This method consists of the use of two rectangular specimens (36.5 cm x 16.5 cm x 2 cm). Three parallel grooves are made in one of the specimens. The hot wire passes through the first groove, and two ECIL brand K/Chromel-Alumel thermocouples pass through the other two grooves, which are positioned 5 mm and 20 mm from the hot wire [40, 41, 42]. The second board was superimposed over the board on which the thermocouples were positioned. Then, a constant electric current passes through the wire, and the variation of the temperature difference between the points at a distance as a function of time is recorded. To heat the sample evenly, it was decided to use a high electrical resistance wire in which the heating takes place by the Joule effect, and it was necessary to lower the voltage level so that the resistance would not cause a short circuit.

Thus, a VARIAC variable autotransformer was used, and a 220 V to 110 V transformer was attached at the output of the VARIAC. The high-resistance wire was coupled to the output of this second transformer in which the Joule effect occurred [41]. After the sample reached a stationary temperature, any temperature variation was detected by both thermocouples. From the data collected, curves of the temperature variation measured by the thermocouples (K) were plotted as a function of time (s).

2.7 Radar chart

Five variables were defined in Table 3, including the vertical flammability, horizontal flammability, mechanical compression, acoustic characteristics, and thermal characteristics. In addition three levels, which ranged from 0 (non-efficient) to 2 (efficient), were defined for each variable according to the data collected in the tests performed [43].

Table 3

Parameters for radar chart

Variable	Level		
	0	1	2
Vertical flammability	Greater than 160 s for total combustion.	From 159 s to 140 s for total combustion.	Less than 139 s for total combustion.
Horizontal flammability	Total Combustion	70 mm/min to 100 mm/min	69.9 mm/min to 40 mm/min

Acoustic	Same as reference	Acoustically absorbs at least one frequency	Acoustically absorbs the highest number of frequencies.
Mechanical compression	Material without any resistance, close to zero	0.1 MPa minimum required by the ABNTNBR 8082, 2016 standard	Results above the minimum required by the standard
Thermal	Less than 14.9 °C	15 to 24.9 °C	Greater than 25 °C

3 Results and Discussion

3.1 Composites

PU was used as the composite matrix due to its established use for thermal and acoustic insulation in buildings. The composites were obtained by the reaction between toluene-2,6-diisocyanate and polypropylene glycol, with the addition of cement, sand, and AAS or GLA [6, 44, 45]. Thus, the composite boards were prepared. Fig. 4 shows the PuCemGla specimen.

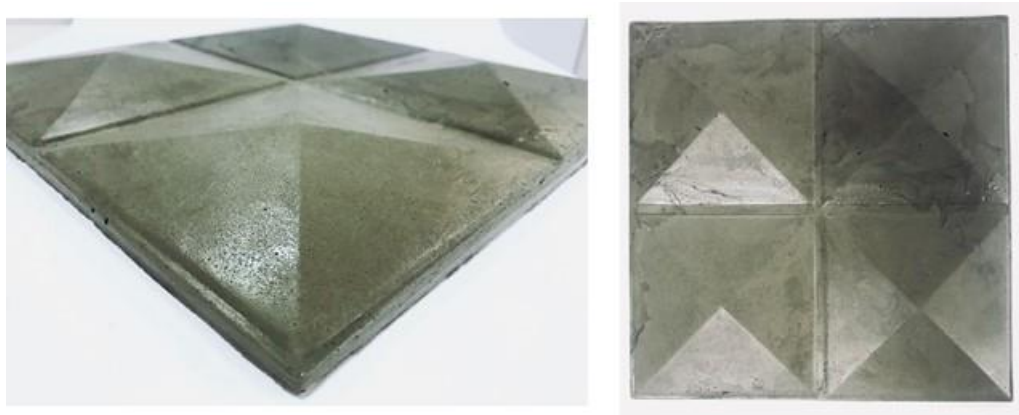


Figure 4. Boards made of PuCemGla composite with length and width of 29.5 cm².

3.2 Scanning electron microscopy, chemical composition and morphological analysis of the image

Fig. 5 shows SEM images of the PuCemAas, PuCemGla, PuCemSan and PuCem composites with 50 × magnification (Fig. 5A, B, C and D), 100 x magnification (Fig. 5A', B',

C' and D'), 200 x magnification (Fig. 5A'', B'', C'' and D'') and another magnification (Fig. 5A''', B''', C''' and D''') [6, 44, 45].

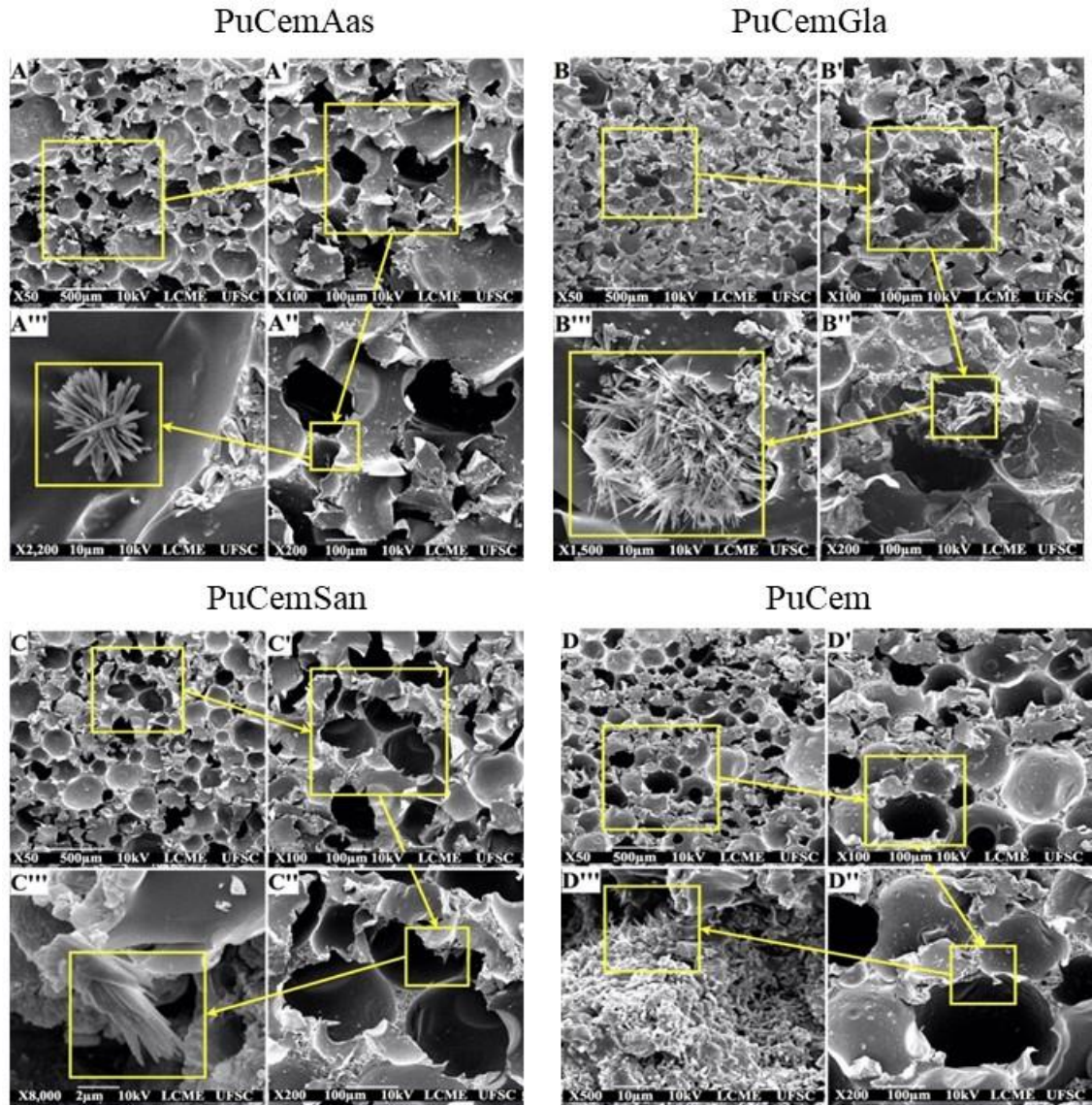


Figure 5. SEM images of the rigid foams: PuCemAas, PuCemGla, PuCemSan and PuCem composites with 50 x magnification (A, B, C and D), 100 x magnification (A', B', C' and D'), 200 x magnification A'', B'', C'' and D'') and another magnification (A''', B''', C''' and D''').

The micrographs of PuCemAas, PuCemGla, PuCemSan and PuCem in Fig. 5 show a cellular structure for all composites and that the open and closed pores were approximately spherical (Fig. 5A, A', A'', B, B', B'', C, C', C'', D, D', D'') [6, 44, 45,46].

The collapse of the cell system occurred for all specimens, and it was possible to visualize the formation of needle-shaped crystals (Fig. 5 A''', B''', C''', D''') on the walls of the PU matrix. Ca(OH)₂ hexagonal crystals were not observed in the micrographs. For all specimens, the chemical composition of the crystals shown in Fig. 5 A''', B''', C''', D''' was determined by EDS and is presented in Table 4 as percentages.

Table 4

Energy-dispersive X-ray spectroscopy of PuCemAas, PuCemGla, PuCemSan and PuCem.

Chemical element (%)	PuCemAas	PuCemGla	PuCemSan	PuCem
C	61.46±1.57	69.27±0.89	75.54±0.81	84.82±1.45
N	7.82±2.84	9.08±2.65	9.95±3.08	-
O	18.92±0.72	6.55±0.57	10.6±0.65	11.46±0.89
Mg	-	-	-	0.12±0.04
Na	0.93±0.06	-	0.11±0.2	-
Al	8.97±0.13	0.15±0.05	0.15±0.02	0.11±0.04
Si	1.21±0.11	1.44±0.11	0.99±0.05	1.98±0.10
K	0.19±0.05	-	0.19±0.03	-
Ca	0.46±0.05	13.50±0.36	2.47±0.09	1.50±0.16
Total	100.00	100.00	100.00	100.00

The samples characterized by EDS consisted mainly of the cementitious portion, but these were dispersed in the PU matrix. In the samples, there were high percentages of the chemical elements C, N and O. High Al and Si percentages were observed for PuCemAas (Table 4), while low percentages of Al and Ca were found for PuCemSan. The percentage of Ca for PuCemGla seems quite high, and the percentages of Si are comparable to those in PuCemAas. Thus, it is suggested that the hydration reaction of the cement without/with nanoparticles of AAS, SAN and GLA formed calcium silicate hydrate, calcium aluminate hydrate and calcium silicate aluminate hydrate, and the calcium can be replaced by another cation, e.g., potassium, sodium or magnesium, according to the EDS [46, 47, 48].

The characterization of the specimens was supplemented by an analysis of the FTIR spectra in Fig. 6.

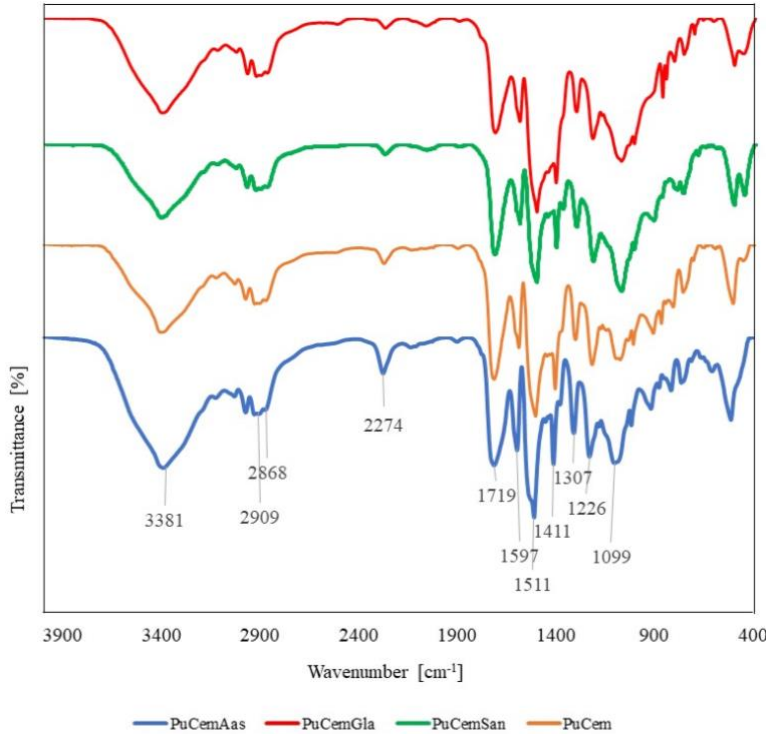


Figure 6. FTIR spectra of PuCem (PU and cement), PuCemAas (PU, cement and AAS), PuCemSan (PU, cement and sand) and PuCemGla (PU, cement and glass sludge).

In the spectra of Fig. 6, the specimens had a wide displacement range of 3690-3120 cm⁻¹, which included the axial deformation vibrations of the N-H of the amides associated with O-H (3380 cm⁻¹), hydroxides (calcium hydroxide at 3645 cm⁻¹), aluminium hydroxide (at 3620 cm⁻¹ for nanocrystals and 3527 cm⁻¹ for amorphous) and water [44, 49, 50]. They also have two absorption bands at 2909 cm⁻¹ and 2868 cm⁻¹ (C-H ethylene elongation, CH₂). In the region close to 2270 cm⁻¹, there is a band associated with the axial deformation vibrations of the accumulated double bonds (N=C=O), and in the region of 1720 cm⁻¹, there is a deformation vibration band of the urethane group (NHCOO).

The presence of benzene rings in the composites was identified by the deformation vibrations of the C=C group at 1600 cm⁻¹ and 1510 cm⁻¹. The angular deformation of the aliphatic C-H was observed at approximately 1411 cm⁻¹ and 1307 cm⁻¹ for the methylene group and methyl group, respectively, and it was observed at 1226 cm⁻¹ for the asymmetrical axial deformation (NHCOO) and at 1099 cm⁻¹ for the asymmetric axial deformation of ether. The band characteristics of Si-O, Al-O and CO₂⁻³ have wavelengths lower than 1000 cm⁻¹, and the absorption bands are attributed to the atomic frequencies of the bond (Si, Al)-O that binds the oxygen atom of the tetrahedron [(Si, Al)O₄]⁻⁴ to the Si atom or to the central Al [41]. The peaks at 815 cm⁻¹ are for Al-O (Al=O slope) (Costa et al., 1999), the O-CaO bending vibrations are at 875 cm⁻¹, and the peak near 510 cm⁻¹ (deformation angle 0) is for the bending vibrations of Al-OH and Ca-OH (Tabelin et al., 2017; Ram, 2001).

The replacement of part of the cement (24.5%) of the initial composition (PuCem) with sand (PuCemSan), aluminium-anodising sludge (PuCemAas) or sludge from glass cutting and polishing (PuCemGla) caused changes in the morphology of the rigid foams. The SEM images of the specimens with a magnification of 50 × Fig. 5 A, B, C, D) were treated using FIJI ImageJ software and produced the corresponding images of Fig. 7 A, B, C, D, A', B', C', D', A'', B'', C'', D'' that were used to define the morphological parameters.

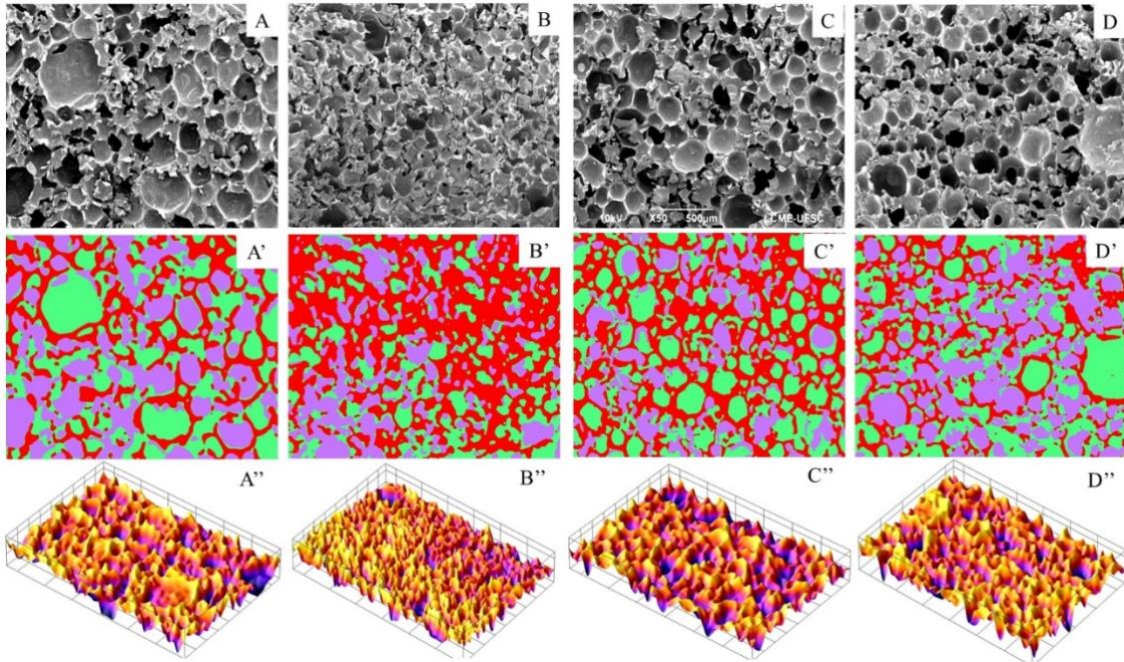


Figure 7. FIJI ImageJ computerized treatment of the SEM surfaces with a magnification of 50 \times of PuCemAas (A, A' and A''), PuCemGla (B, B' and B''), PuCemSan (C, C' and C'') and PuCem (D, D' and D'').

The images in Fig. 7A, B, C, D were generated by filters to obtain a higher contrast of the edges and alveoli; in the images of Fig. 7A', B', C', D', one can find the surface cutting edges (red, class 1), shallow alveoli (green, class 2) and deep and perforated alveoli (lilac, class 3) [20]. From this classification, it was possible to generate the topography of the images in Fig. 3 A'', B'', C'', D'', where the top regions are shown in bright colour and the low regions in dark colour.

The intervals of the area means and circularities for each class with the standard deviations and 95% confidence intervals were calculated for Figs. 7A', B', C' and D', and the results are shown in Fig. 8 and Fig. 9, respectively.

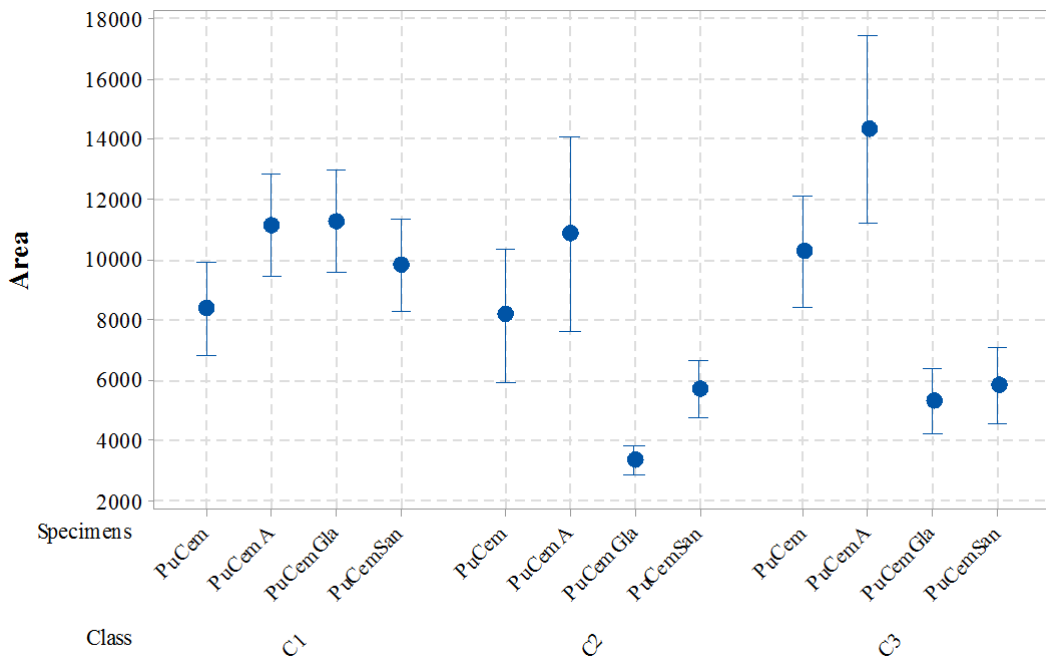


Figure 8. Ranges of area means (μm^2) for classes 1, 2, and 3 of PuCemAas (Fig. 7 A'), PuCemGla (Fig. 7 B'), PuCemSan (Fig. 7 C') and PuCem (Fig. 7 D') with 95% confidence intervals.

In Fig. 8, for class 1, the surface cutting edges of the composites showed similar areas; that is, they do not show differences when observed by the confidence intervals and have a similar dispersion for each specimen. For class 2, shallow alveoli, the areas showed variations, where the PuCem area was similar to the PuCemAas area. For class 3, deep and perforated alveoli, the PuCem and PuCemAas areas were similar but distinct from those of PuCemGla and PuCemSan, which were similar to each other. For classes 2 and 3, PuCemGla and PuCemSan have lower dispersions when compared with PuCem and PuCemAas.

The intervals of the circularity mean values (Fig. 9) were calculated from the images in Fig. 7A', B', C' and D' for each class with the standard deviations and 95% confidence intervals.

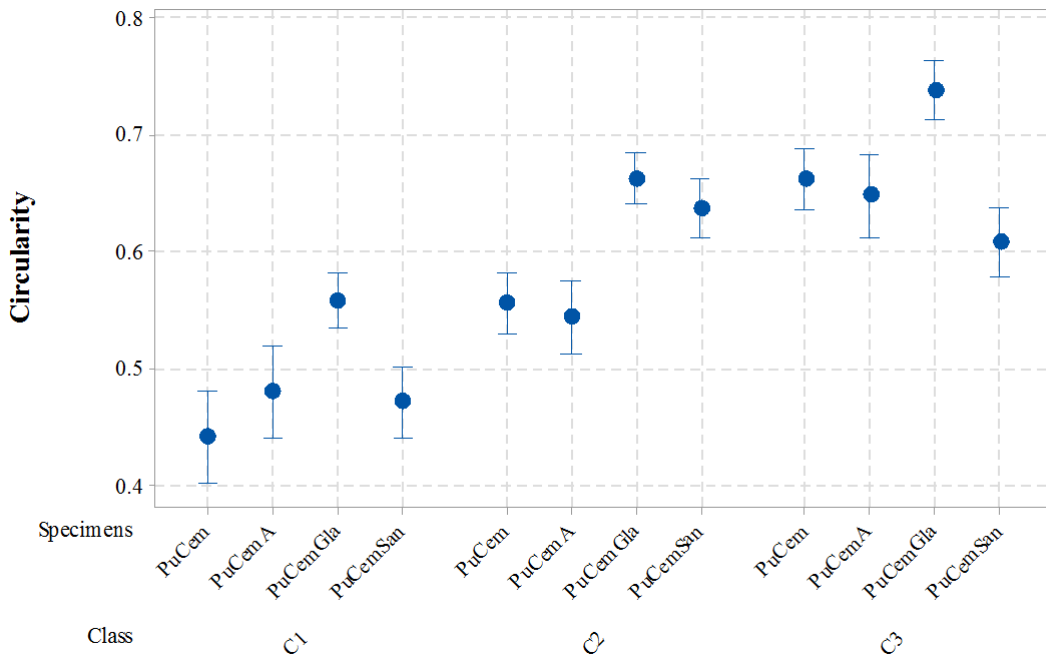


Figure 9. Mean circularity intervals for classes 1, 2, and 3 of PuCemAas (Fig. 3 A'), PuCemGla (Fig. 7 B'), PuCemSan (Fig. 7 C') and PuCem (Fig. 7 D'), with confidence intervals of 95%.

The circularity can range from 0 to 1, where 0 is for an elongated area and 1 is for a circular area. In Fig. 9, it was observed for class 1 that the mean circularity was, in general, less than 0.5, which indicates more elongated areas. For class 2, the circularity was greater than 0.5, with a low dispersion (small CIs), and the composites PuCemGla and PuCemSan are similar to each other and present greater circularities than PuCem and PuCemAas, which are also similar to each other. For class 3, the circularities were greater than 0.6 with a low dispersion (small CIs), and the PuCemGla composite showed greater circularity than the other specimens.

The ANOVA-Tukey tests for the areas and circularities of the alveoli (class 2 and 3) enabled the analysis of whether the areas and the circularities were equal or significantly different. ANOVA was used to verify the existence of a difference between the means (Fig. 10), and the Tukey test was used to verify which of the composites presents a significant difference of means (Fig. 11). Fig. 10 shows the means of the areas (μm^2) and the circularities

for the alveoli (classes 2 and 3) of PuCemAas (Fig. 7 A'), PuCemGla (Fig. 7 B'), PuCemSan (Fig. 7 C') and PuCem (Fig. 7 D'), with confidence intervals of 0.95.

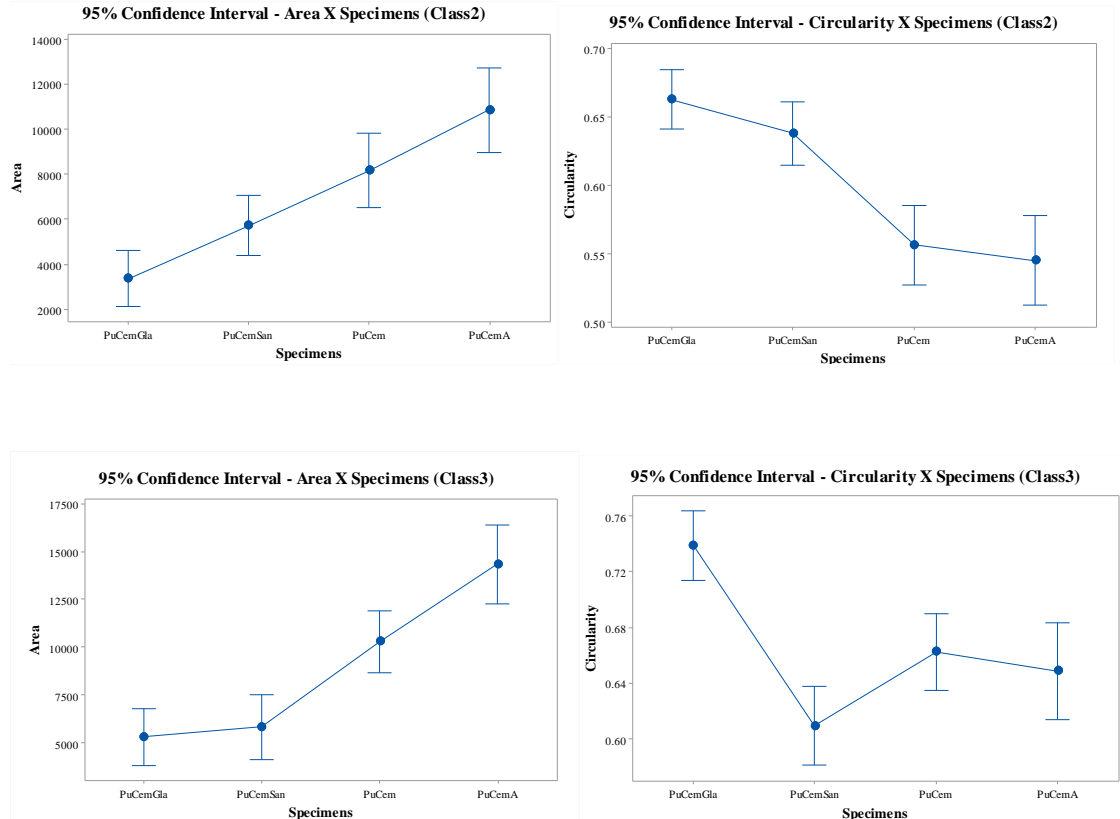


Figure 10. Graphs of the means of the areas (μm^2) and circularities for the alveoli (classes 2 and 3) of PuCemSan, PuCemGla, PuCemAas and PuCem with confidence intervals of 0.95.

Fig. 10 shows graphs of the means of the areas and circularities with 95% confidence intervals for the composites; the ANOVA tests (Fig. 10) provide an experimental value of F-Snedecor greater than 16, which led to p-values very small and close to zero. Thus, in all cases, at a significance level of $0.05/2 = 0.025$ (two-tailed test), not all means are equal, i.e., at least one of the means of the area or circularity is significantly different from the other values (alternative hypothesis).

In Fig. 10, it can be observed that there are actually significant differences between some of the areas and the circularities, both for the class 2 alveoli and for the class 3 alveoli of the

composites. To define the significance of the differences between the areas and the circularities, Tukey's pairwise comparison test and Tukey's simultaneous test were performed. Fig. 11 shows the results of the Tukey tests for the differences of the means for the areas and circularities of classes 2 and 3 of the composites.

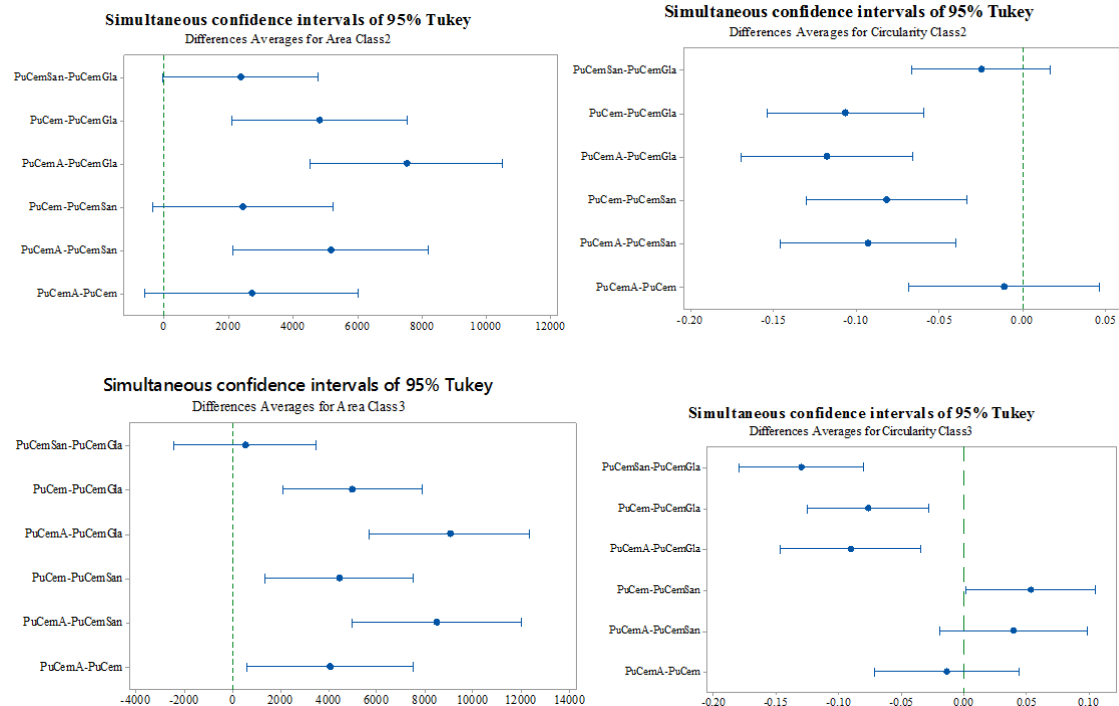


Figure 11. Tukey tests for the differences of the means for the areas and circularities of classes 2 and 3 of PuCemSan, PuCemGla, PuCemAas and PuCem.

Thus, the ANOVA-Tukey tests of the composites showed that the class 2 alveoli in the PuCemAas and PuCemGla areas are significantly different from each other and the other composites and that the composites have significantly different circularities. For the Class 3 alveoli, the areas of the PuCemAas composites are significantly different from those of the PuCemGla and PuCemSan composites, but the latter two are similar to each other. PuCem and PuCemAas have similar areas to PuCem and PuCemGla and PuCem to PuCemGla. Regarding

the circularity, the composites PuCemGla and PuCemSan are significantly different from PuCem and PuCemAas (which are similar to each other).

3.3 Mechanical compressive strength

Fig. 12 shows the stress-strain behaviour of the PuCem, PuCemAas, PuCemSan and PuCemGla composites.

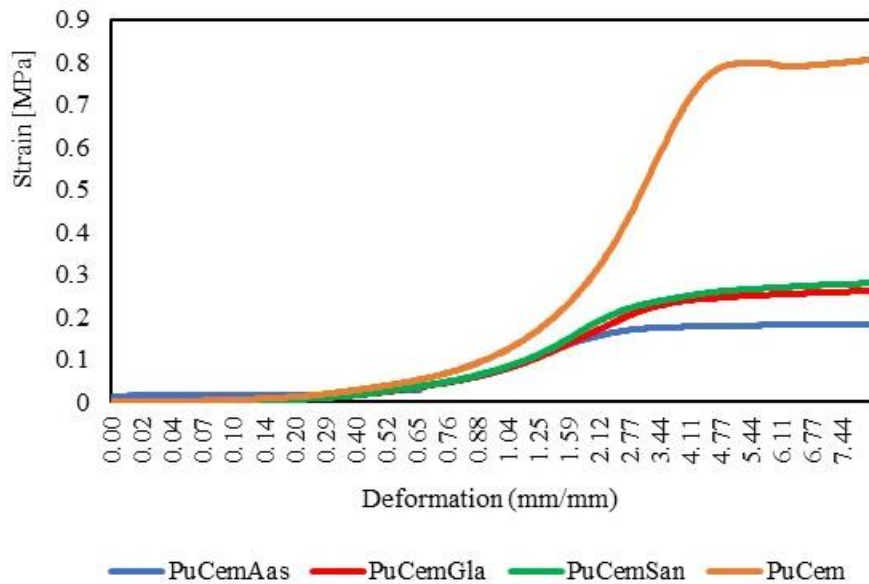


Figure 12. Compressive strengths of PuCem, PuCemAas, PuCemSan and PuCemGla.

In Fig. 12, the initial compressive strength stage was elastic, followed by a plastic deformation, typical of rigid PU foams. The best result for the ultimate compressive stress was obtained for the PuCem composite, 0.8 MPa, which was probably due to the covalent coordinate bonds between the calcium-silicate-hydrate groups and PU [7]. For the other composites, there was a reduction of 0.6 to 0.7 MPa in the ultimate stress. By replacing 24.5% of the cement with sand, AAS or GLA the cement cure and formation of aluminates and silicates were affected. The metal oxides in greater quantity SiO_2 and AlO_2 , acted as fillers,

breaking the existing bonds in the PU but not compensating for the formation of aluminates and silicates with the cement [6, 41, 47, 48].

Furthermore, it can be observed that the compressive strength behaviours of PuCemSan and PuCemGla were similar, even when containing different sizes of SiO₂ nanoparticles, sand particles smaller than 150 μm and glass sludge particles smaller than 45 μm; however, according to the ANOVA-Tukey tests, these composites are significantly similar regarding the circularity of the alveoli (class 2) and the alveolar area (class 3). It should also be mentioned that a lower value was found for the compressive strength exhibited by PuCemAas, with the AAS particles smaller than 45 μm, which had a circularity significantly similar to that of the PuCem circularity but an area that was not significantly different but greater than those of the other composites (classes 2 and 3).

Thus, in addition to the intermolecular interactions in the materials, the influence of the morphology of the material can also be observed to a lesser degree because the PuCem exhibited intermediate alveolar areas (classes 2 and 3), greater than those of PuCemSan and PuCemGla but smaller than those of PuCemAas. The maximum compressive strength was greater than 0.1 MPa for all composites, and rigid polyurethane foam must withstand a compressive strength of 0.1 MPa (100 kPa) to be used as an insulating material between walls [49].

3.4 Thermal stability and flammability

In a fire, some of the material undergoes non-oxidizing thermal degradation, and some of the material undergoes oxidizing degradation (combustion). For PU, non-oxidizing thermal degradation reactions were reported at temperatures above 300°C, and the tested specimens

showed similar behaviour [52]. Fig. 13 shows the DTA/TGA thermograms of PuCem, PuCemGla, PuCemSan, PuCemAas and PuCemATH.

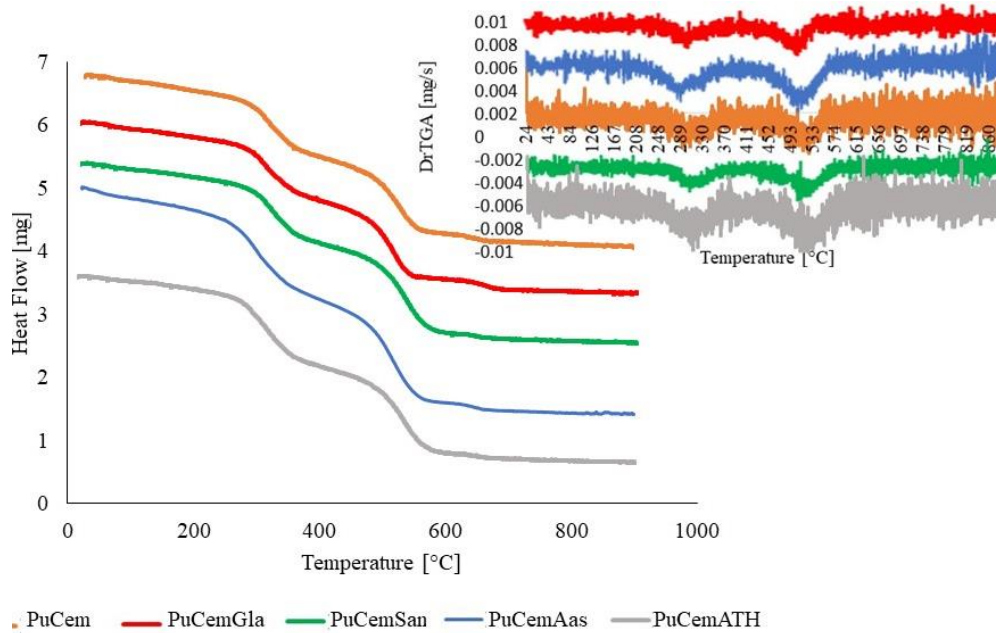


Figure 13. DTA/TGA thermograms of PuCem, PuCemGla, PuCemSan, PuCemAas and PuCemATH.

The DTA/TGA thermograms of the specimens show two levels of endothermic decomposition, with PuCemATH at 292.15°C (28.60%) and 519.39°C (31.85%), PuCem at 298.41°C (26.16%) and 507.73°C (27.88%), PuCemAas at 290.09°C (23.85%) and 513.53°C (29.84%), PuCemSan at 302.14°C (23.14%) and 518.57°C (31.76%), and PuCemGla at 291.84°C (17.73%) and 492.11°C (25.57%). In general, the first stage in the endothermic decomposition corresponded to the rupture of the rigid urethane segment, and the second stage corresponded to the thermal decomposition of the flexible segment, the polyol [52,53]. The decomposition temperatures of the composites were similar, and the incorporation of cement, sand, GLA or AAS contributed a maximum of 10°C of thermal stability, in the case of PuCemSan.

The specimens were investigated regarding their behaviour during combustion in the horizontal and vertical directions. Table 5 shows encouraging results regarding the flame retardant effect of the composites.

Table 5

Burning time in the horizontal flammability test.

Composite	Mean t (s) up to 25 mm	Mean combustion time of the specimens (s)	Mean distance travelled by the flame (mm)	Mean speed (mm/min)
PuCem	35.00	45.53	75.00	98.83
PuCemATH	18.67	39.93	28.17	42.33
PuCemAas	18.00	37.83	30.00	47.58
PuCemSan	11.33	42.11	28.67	40.85
PuCemGla	12.00	68.00	91.67	80.88

In Table 5, PuCem showed combustion with a burning rate of 98.83 mm/min, while the burning rates of PuCemAas, PuCemSan and PuCemGla were 47.58 mm/min, 40.85 mm/min and 80.88 mm/min, respectively. PuCemSan showed better results, even when compared to the PuCemATH specimen containing a commercial flame retardant. In this test, it should be noted that the sample is positioned perpendicularly to the flame, which limits the diffusion of oxygen in the solid phase. Furthermore, the combustion gases do not directly reach the solid surface, which reduces the propagation of the flame [52, 54]. These results are mainly attributed to the presence of oxides, silicates and aluminates (GLA, AAS, sand and cement), which, in addition to not combusting, can also form a ceramic layer due to the temperature reached during combustion preventing the flame from propagating. Video 1 shows the horizontal flammability test for PuCemGla and PuCemAas.

In the vertical flammability test, the sample remains in the direction of the flame propagation. Table 5 shows the duration of the flaming combustion of the five specimens and the classification according to the flammability of the vertical combustion [37].

Table 5

Combustion time and classification for the vertical flammability test for PuCem, PuCemATH, PuCemAas, PuCemSan and PuCemGla.

Composite	Burning time for the specimens (s)					Total	Rating
	1	2	3	4	5		
PuCem	27.00	22.00	32.00	39.00	30.00	150.00	Not applicable
PuCemATH	8.75	8.77	11.50	9.00	14.00	52.02	V1
PuCemAas	34.48	26.83	24.45	29.49	22.31	137.56	Not applicable
PuCemSan	32.15	28.07	23.69	29.68	27.03	140.62	Not applicable
PuCemGla	28.29	32.00	39.00	30.5	35.57	165.36	Not applicable

The specimens had a total combustion time of less than 250 s for each series of 5 samples. With the exception of PuCemATH, the specimens burned to the fastener and did not meet the vertical flammability classification. Although no sample reached the vertical flammability classification, the samples were able to decrease the propagation of the flame in the horizontal position [6, 7, 52].

3.5 Acoustic Testing

Fig 14. shows the curves of the sound intensity level obtained for ten frequencies ranging from 0 Hz to 16000 Hz for PuCem, PuCemGla, PuCemSan, PuCemAas and the composite without PU.

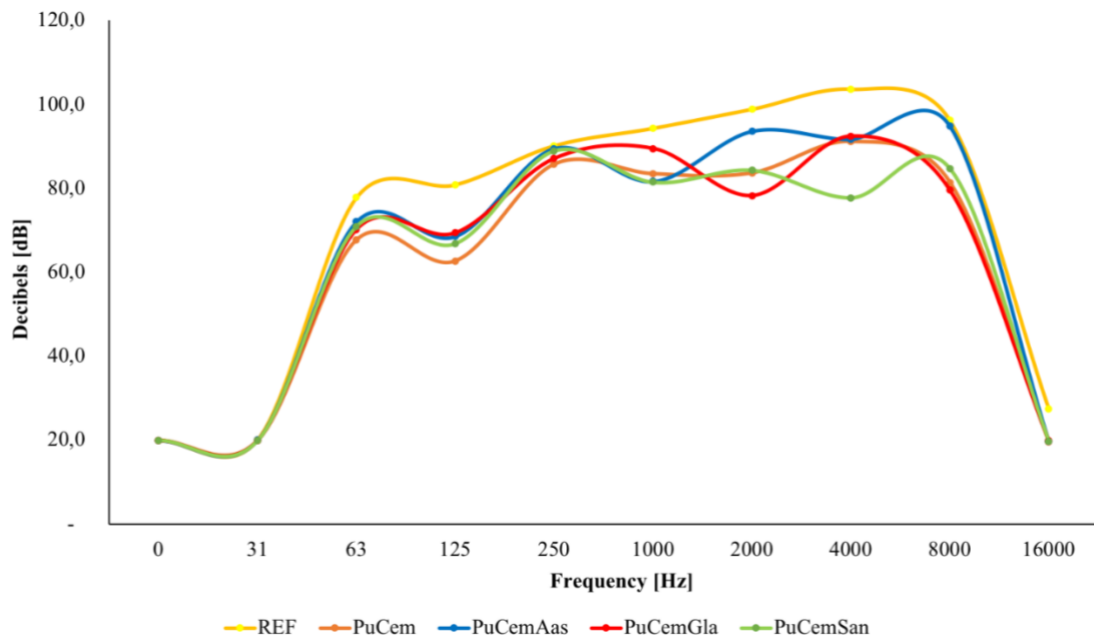


Figure 14. Curves of sound intensity levels as a function of the frequency from 0 Hz to 16000 Hz.

The air flow resistivity and porosity are fundamental properties of acoustic materials that affect their noise absorption. The composites showed no differences at the frequencies of 0 Hz, 31 Hz, 250 Hz and 16000 Hz (Fig. 14). However, they did offer a sound barrier, reducing the sound intensity by up to 10.1 dB, 18.2 dB, 12.9 dB, 20.6 dB, 25.9 dB, 15.3 dB at frequencies of 63 Hz, 125 Hz, 1000 Hz, 2000 Hz, 4000 Hz and 8000 Hz, respectively, relative to the measurements without the PU composite (REF curve) [55]. The composites had alveoli with a high circularity greater than 0.5 (relative to 1 for circular areas); thus, the energy can be dissipated by the reflection of the wave in the alveoli.

PuCemSan presented a higher sound absorption at frequencies of 1000 Hz and 4000 Hz, while PuCemGla presented a higher sound absorption at frequencies of 2000 Hz and 8000 Hz. These have small alveolar areas (classes 2 and 3) in relation to the other composites and good circularity (between 0.6-0.8). In the ANOVA-Tukey tests, PuCemGla and PuCemSan were significantly similar.

3.6 Heat capacity by hot wire method

Fig. 15 shows the temperature variation curves as a function of time for PuCem, PuCemGla, PuCemSan and PuCemAas.

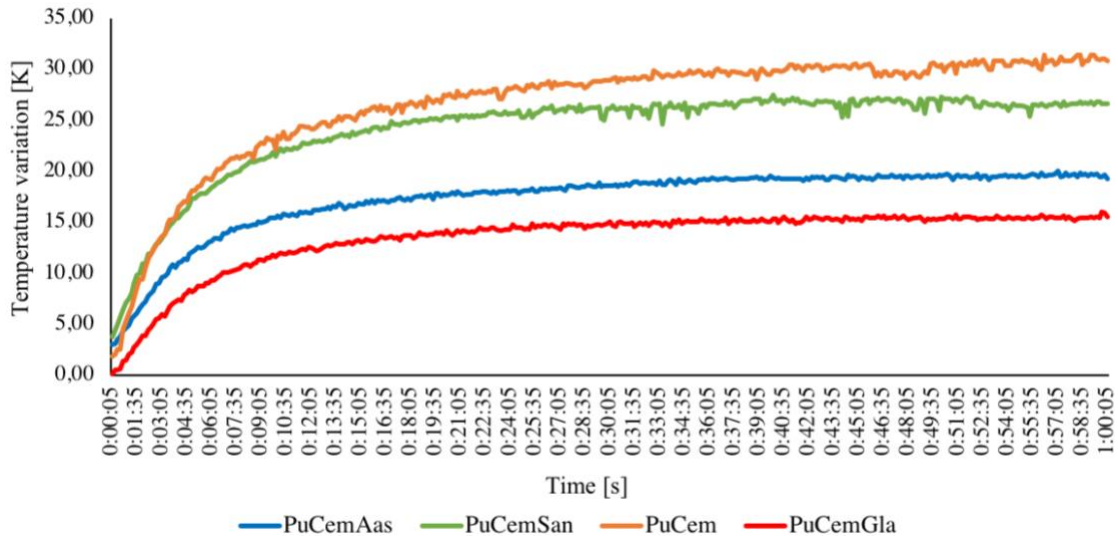


Figure 15. Variation of the temperature (K) as a function of time (s) for PuCem, PuCemGla, PuCemSan and PuCemAas.

Fig. 15 shows measurements of the temperature variation as a function of time using the hot wire method, demonstrating the thermal behaviour of the materials when exposed to a heat source. The results indicated that PuCemAas and PuCemGla were better thermal insulators than PuCemSan and PuCem. Thus, the thermal acoustic boards produced from mixtures with GLA and AAS offered higher thermal resistance than the boards without the waste [40, 42].

The thermal behaviour of the composites did not depend only on the composition, as the thermal conductivity for Al_2O_3 (the main constituent of AAS) is higher ($30 \text{ Wm}^{-1}\text{K}^{-1}$) than the thermal conductivities of SiO_2 ($1.3 \text{ Wm}^{-1}\text{K}^{-1}$), mortar ($0.70 \text{ Wm}^{-1}\text{K}^{-1}$) and rigid polyurethane foam ($0.025\text{-}0.035 \text{ Wm}^{-1}\text{K}^{-1}$). The behaviour of the composites can be attributed to the presence of the alveoli (Fig. 5). The statistical analyses performed using the ANOVA-Tukey

tests showed that the medium depth alveoli of the composites containing waste are significantly different from each other and the composites without the presence of waste. These characteristics may have led to changes in the thermal behaviour of the materials.

3.7 Radar chart

Figure 16 shows a radar chart in which five variables – vertical flammability, horizontal flammability, acoustic test, mechanical compression and thermal characteristics – were analysed at three levels, ranging from 0 for non-efficient to 2 for efficient.

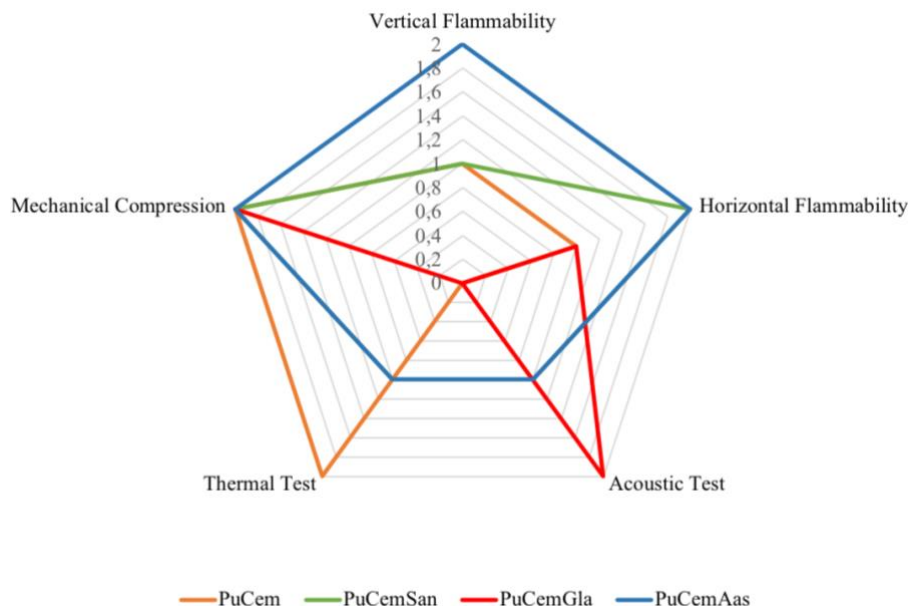


Figure 16. Radar chart where variables - vertical flammability, horizontal flammability, acoustic test, mechanical compression and thermal characteristics - were analysed at levels ranging from 0 for non-efficient to 2 for efficient –.

A comparison between the composites was performed (Fig. 16), and PuCemAas showed the best result, as it reached a maximum score in 3 of the 5 items analysed, namely, vertical and horizontal flammability and the mechanical strength test, as well as a mean score for the acoustic and thermal tests. PuCemSan obtained the maximum score in Horizontal Flammability and Mechanical Compression and an average score in the Thermal Test, Acoustic Test and

Vertical Flammability. PuCem had maximum scores in the Mechanical Compression and Thermal Tests, an average score in Vertical Flammability, and a minimum score in the Acoustic Test. PuCemGla obtained the maximum score in the Acoustic Test and Mechanical Compression, an average score in Horizontal Flammability and minimum scores in the Thermal Test and Vertical Flammability. Thus, the composite with the highest score was the one with the best result.

4. Conclusions

PU composites were prepared with cement, sand, GLA and AAS. This study demonstrates that these inputs can be used as raw materials for the production of boards for civil construction. SEM showed that the replacement of cement with sand or wastes maintained the alveolar structure, but there was a reduction in the mechanical strength of the rigid foams. The composites developed in the study were resistant to horizontal propagation but not to vertical flame propagation according to [37]. The composites showed no significant differences in the sound barrier behaviour at less than 250 Hz or more than 16000 Hz but acted as a sound barrier at frequencies of 1000 Hz, 2000 Hz, 4000 Hz and 8000 Hz. PuCemAas and PuCemGla were better thermal insulators than PuCemSan and PuCem.

The PuCemSan composite presented three superior results: horizontal flammability, acoustic characteristics and mechanical compression, followed by PuCemAas, highlighting the good results in the flame propagation tests. Thus, the AAS is a technically feasible alternative to reduce the use of raw materials from non-renewable sources. More studies are recommended to meet these demands. The limitations of this study include the lack of cost estimates and an economic feasibility analysis for the large-scale production of these boards.

Acknowledgments

We thank HUBER Raw Material (SP, Brazil), Personal glass (SC, Brazil) and Hydro (SC, Brazil) for the donation of ATH, GLA and AAS, respectively. This work was supported by the Foundation of Amparo to the Research and Innovation of the State of Santa Catarina [No 09/2015, Research Group on Science, Technology and Innovation in Materials and No. 06/2017, Research Group on Active Materials], Coordination for the Improvement of Higher Education Personnel. We also thank LEC-UNISUL and Hugo Gallardo, PhD, Professor of the Federal University of Santa Catarina (UFSC), for their support of this research. The electron microscopy work was performed with the JEOL JSM-6390LV microscope of the LCME-UFSC and the UNISULVIRTUAL by videos.

References

- [1] Demirel, B., 2013. Optimization of the composite brick composed of expanded polystyrene and pumice blocks. *Construction and Building Materials*, 40, p.306-313. <http://dx.doi.org/10.1016/j.conbuildmat.2012.11.008>.
- [2] Huysmans, S., SchaepeMeester, J., Ragaertb, K., Dewulfa, J., Meester, S., 2017. Performance indicators for a circular economy: a case study on post-industrial plastic waste. *Resources, Conservation and Recycling*, 120, p.46-54. <http://hdl.handle.net/1854/LU-8507928>.
- [3] Keshavarz, Z., Mostofinejad, D., 2019. Porcelain and red ceramic wastes used as replacements for coarse aggregate in concrete. *Construction and Building Materials*, 195, p.218-230. <https://doi.org/10.1016/j.conbuildmat.2018.11.033>.
- [4] Pivnenko, K., Eriksen, M. K., Martín-fernández, J. A., Eriksson, E., Astrup, T. F., 2016. Recycling of plastic waste: presence of phthalates in plastics from households and industry. *Waste Management*, 54, p.44-52. <https://doi.org/10.1016/j.wasman.2016.05.014>.
- [5] Salesa, A., Perez-Benedicto, J.A., Colorado-Aranguren, D., Lopez-Julian, P.L., Esteban, L.M., Sanz-Baldúz, L.J., Saez-Hostaled, J.L., Ramis, J., Olivares, D., 2017. Physico - mechanical properties of multi - recycled concrete from precast concrete industry. *J. Clean Prod.*, 141, p. 248-255. <https://doi.org/10.1016/j.jclepro.2016.09.058>.
- [6] Marques, D.V., Barcelos, R.L., Parma, G.O.C., Girotto, E., Cruz Jr. A., Pereira N.C., Magnago, R.F., 2019. Recycled polyethylene terephthalate and aluminum anodizing sludge-based boards with flame resistance. *Waste Management*, 92, p. 1-14. <https://doi.org/10.1016/j.wasman.2019.05.013>

- [7] Marques, D.V., Barcelos, R.L., Silva, H.R.T., Egert, P., Parma, G.O.C., Girotto, E., Consoni, D., Benavides, R., Silva, L., Magnago, R. F., 2018. Recycled polyethylene terephthalate-based boards for thermal-acoustic insulation. *Journal Cleaner Production*, 189, p.251-252. <https://doi.org/10.1016/j.jclepro.2018.04.069>.
- [8] Silva, H. R. T., Cavalcante, B. M. M., Marques, D. V., Egert, P., Magnago, R. F., Consoni, D. R., Zanco, J. J., 2017. Placas ecoeficientes: aproveitamento de resíduo de EVA em compósitos usados para isolamento acústico. *Mix Sustentável*, 3, p. 42-49. <https://doi.org/10.29183/2447-3073.mix2017.v3.n2.40-47>.
- [9] Souza Jr., Z., Silva, H. R. T., Egert, P., Magnago, R. F., 2017. Valorização de resíduo industrial: estudo acústico de placas eva/cimento. *Mix Sustentável*, v.3, p. 140-141. <https://doi.org/10.29183/2447-3073.mix2017.v3.n1.140-141>.
- [10] Magnago, R.F., Muller, N.D., Martins, M., Silva, H.R.T., Egert, P., Silva, L., 2017. Investigating the influence of conduit residues on polyurethane plates. *Polimeros*. v. 27, n. 3, 23-37. <http://dx.doi.org/10.1590/0104-1428.05616>.
- [11] Barcelos, R.L., Cubas, A.L.V., Dutra, A.R.A., Silva, L., Leripio, A.A., Magnago, R.F., 2016. Preparation of polyurethane sheets using surfboard manufacturing waste and evaluation of their properties to use in Brazil's construction industry. *J. Biol. Chem. Res.* 3, p. 103-120. <http://www.ss-pub.org/wp-content/uploads/2016/05/BCR2016011301.pdf>. (accessed 25 August 2017).
- [12] Palomar, I., Barluenga, G., Puentes, J. Lime–cement mortars for coating with improved thermal and acoustic performance, 2015. *Construction and Building Materials*, 75, p. 306-314. <http://dx.doi.org/10.1016/j.conbuildmat.2014.11.012>.
- [13] Degrave-Lemeurs, M., Glé, P. A., Menibus, H. Acoustical properties of hemp concretes for buildings thermal insulation: application to clay and lime binders. *Construction and Building Materials*, 160, p. 462-474. <https://www.sciencedirect.com/science/article/abs/pii/S0950061817322419>.
- [14] Somarathna, H.M.C.C., Raman, S.N., Mohotti, D., Mutalib, A.A., Badri, K.H. 2018. The use of polyurethane for structural and infrastructural engineering applications: a state-of-the-art review. *Construction and Building Materials*, 190, p. 995-1014. <https://doi.org/10.1016/j.conbuildmat.2018.09.166>.
- [15] Heikal, M., Ismail, M. N, Ibrahim, N.S., 2015. Physico-mechanical, microstructure characteristics and fire resistance of cement pastes containing Al₂O₃ nano-particles. *Construction and Building Materials*, 91, P. 232–242. <https://doi.org/10.1016/j.conbuildmat.2015.05.036>.
- [16] Huang, B., Zhao, J., Chai, J., Xue, B., Zhao, F., Wang, X., 2017. Environmental influence assessment of China's multi-crystalline silicon (multi-Si) photovoltaic modules considering recycling process. *Solar Energy*, 143, p. 132-141. <http://doi.org/10.1016/j.solener.2016.12.038>.
- [17] Lombard, B., Maurel, A., Marigo, J., 2017. Numerical modeling of the acoustic wave propagation across an homogenized rigid microstructure in the time domain. *Journal of Computational Physics*, 335, p. 558-577. <http://doi.org/10.1016/j.jcp.2017.01.036>.
- [18] Quan, L., Sounas, D., Alu, A. 2017. Non-reciprocal sound propagation in zero-index metamaterials. *Journal of the Acoustical Society of America*, 141, p. 3698. <https://doi.org/10.1121/1.4988062>.

- [19] Kinnane, O., Reilly, A., Grimes, J., Pavia, S., Walker, R. 2016. Acoustic absorption of hemp-lime construction. *Construction and Building Materials*, 122, 674-682. <https://doi.org/10.1016/j.conbuildmat.2016.06.106>.
- [20] Zhu, H., Xu, S., 2019. Synthesis and properties of rigid polyurethane foams synthesized from modified urea-formaldehyde resin. *Construction and Building Materials*, 202, p. 718-726. <https://doi.org/10.1016/j.conbuildmat.2019.01.035>.
- [21] Liu, G., Florea, M.V.A., Brouwers, H.J.H. 2019. Performance evaluation of sustainable high strength mortars incorporating high volume waste glass as binder. *Construction and Building Materials*, 202, p. 574- 588. <https://doi.org/10.1016/j.conbuildmat.2018.12.110>.
- [22] Chu, L., Fwa, T.F., 2019. Functional sustainability of single- and double-layer porous asphalt pavements. *Construction and Building Materials*, 197, p. 436-443. <https://doi.org/10.1016/j.conbuildmat.2018.11.162>.
- [23] Hossain, M.U., Poon, C.S., 2018. Global warming potential and energy consumption of temporary works in building construction: a case study in Hong Kong. *Building and Environment*, 142, p. 171-179. <https://doi.org/10.1016/j.buldenv.2018.06.026>.
- [24] Shams, A., Stark, A., Hoogen, F., Hegger, J., Schneider, H. 2015. Innovative sandwich structures made of high performance concrete and foamed polyurethane. *Composite Structures*, 121, p. 271–279. <https://doi.org/10.1016/j.compstruct.2014.11.026>.
- [25] Garrido, M., Correia, J.R., Keller, T., 2016. Effect of service temperature on the shear creep response of rigid polyurethane foam used in composite sandwich floor panels. *Construction & Building Materials*, 18, 235-244. <http://dx.doi.org/10.1016/j.conbuildmat.2016.05.074>.
- [26] Thirumal, M., Khastgir, D., Singha, N. K., Manjunath, B. S., Naik, Y. P., 2007. Mechanical, morphological and thermal properties of rigid polyurethane foam: effect of the fillers. *Cellular Polymers*, 26, p. 245-259. <https://doi.org/10.1177/026248930702600402>.
- [27] Vladimirov, V.S., Lukin, E.S., Popoya, N.A., Ilyukhin, A., Moizis, S.E., Artamonov, M.A. 2011. New types of light-weight refractory and heat-insulation materials for long-term use at extremely high temperatures. *Glass and Ceramics*, 68, n.3-4, p.116-122. <https://doi.org/10.1007/s10717-011-9335-7>.
- [28] Malaiškienė, J., Vaičienė, M., Žurauskienė R., 2011. Effectiveness of technogenic waste usage in products of building ceramics and expanded clay concrete. *Construction and Building Materials*, 25, p. 3869–3877. <https://doi.org/10.1016/j.conbuildmat.2011.04.008>.
- [29] Miranda, J. I., *Processamento de Imagens Digitais*: métodos multivariados em JAVA. Brasília: Embrapa Informação Tecnológica, 2011.
- [30] Sanches, C.H., Fontoura, P.J., Vieira, P.F., Batista, M.A., Técnicas de suavização de imagens e Eliminação de ruídos. Encontro Anual de Tecnologia da Informação e Semana Acadêmica de Tecnologia da Informação, 4, 2005. *Anais...* Frederico Westphalen, Rio Grande do Sul. p.21-30. <http://eati.info/eati/2015/assets/anais/Longos/L2.pdf> (accessed 28 August 2017).
- [31] Centro Estadual de Pesquisas em Sensoriamento Remoto e Meteorologia (CEPSM). Página dinâmica para o aprendizado de Sensoriamento Remoto: técnicas de manipulação de imagens. <http://www.ufrgs.br/engcart/PDASR/maniphist.html> (accessed 28 August 2017).

- [32] Instituto Nacional de Pesquisas Espaciais, Divisão de Processamento de Imagens (INPE). Spring: tutorial de geoprocessamento. Filtragem.
<http://www.dpi.inpe.br/spring/teoria/filtrage/filtragem.htm> (accessed 28 August 2017).
- [33] Facon, J., *Morfologia Matemática*: teoria e exemplos. Curitiba: Editora Universitária Champagnat PUC, 1996.
- [34] Larson, R., Farber, E., *Estatística aplicada*. 4 ed. São Paulo: Pearson Prentice Hall, 2010.
- [35] American Society for Testing and Materials - ASTM. ASTM D1621-16: *Standard test method for compressive properties of rigid cellular plastics*, ASTM. 2010.
- [36] American Society for Testing and Materials - ASTM. ASTM D618-13: *Standard practice for conditioning Plastics for testing*, ASTM. 2013.
- [37] Underwriters Laboratories, 2017. *Test for Flammability of plastic materials for parts in devices and appliances*. UL 94. 2017
- [38] American Society for Testing and Materials - ASTM. ASTM D635-14: *Standard test method for rate of burning and/or extent and time of burning of plastics in a horizontal position*. ASTM. 2014.
- [39] American Society for Testing and Materials - ASTM. ASTM D3801-10: *Standard test method for measuring the comparative burning characteristics of solid plastics in a vertical position*. ASTM. 2010
- [40] Sacht, H.M., Rossignolo, J. A., Santos, W.N., 2010. Avaliação da condutividade térmica de concretos leves com argila expandida. *Revista Materia*, v. 15, n. 1, p. 31-39.
<http://www.materia.coppe.ufrj.br/sarra/artigos/artigo11099> (accessed 28 August 2018).
- [41] Santos, W.N., 2002. O método de fio quente: técnica em paralelo e técnica de superfície. *Cerâmica*, 48, p. 86-91. <http://dx.doi.org/10.1590/S0366-69132002000200007>.
- [42] Carvalho, G., Frollini, E., Santos, W.N., 1996. Thermal conductivity of polymers by hot-wire method. *Journal of Applied Polymer Science*, 62, p. 2281-2285.
[https://doi.org/10.1002/\(sici\)1097-4628\(19961226\)62:13%3c2281::aid-app12%3e3.0.co;2-6](https://doi.org/10.1002/(sici)1097-4628(19961226)62:13%3c2281::aid-app12%3e3.0.co;2-6).
- [43] Kovacic, I., Waltenbereger, L., Gourlis, G., 2016. Tool for life cycle analysis of facade-systems for industrial buildings. *Journal of Cleaner Production*, 130, p. 260-272.
<https://doi.org/10.1016/j.jclepro.2015.10.063>.
- [44] Wang, Y., Wang, F., Dong, Q., Xie, M., Liu, P., Ding, Y., Zhang, S., Yang, M., Zheng, G. 2017. Core-shell expandable graphite @ aluminum hydroxide as a flame-retardant for rigid polyurethane foams. *Polym. Degrad Stabil.* 146, 267-276.
<https://doi.org/10.1016/j.polymdegradstab.2017.10.017>.
- [45] Zhang, X.L., Duan, H.J., Yan, D.X., Kang, L.Q., Zhang, W.Q., Tang, J.H., Li, Z. M., 2015. A facile strategy to fabricate microencapsulated expandable graphite as a flame-retardant for rigid polyurethane foams. *J. Appl. Polym. Sci.*, 132, p. 42364.
<https://doi.org/10.1002/app.42364>.
- [46] Vaičiukynienė, D., Skipkiūnas, G., Sasnauskas, V., Daukšys, M. Cement compositions with modified hydrosodalite. *Chemija*. 2012. v. 23. n. 3. p. 147-154.
<http://mokslozurnalai.lmaleidykla.lt/publ/0235-7216/2012/3/147-154.pdf>. (accessed 30 August 2018).

- [47] Kunther, W., Ferreiro S., Skibsted J., 2017. Influence of the Ca/Si ratio on the compressive strength of cementitious calcium–silicate–hydrate binders. *Journal of Materials Chemistry A. J. Mater. Chem. A*, 5, p. 17401-17412. <https://doi.org/10.1039/c7ta06104h>.
- [48] Heikal M., Ismail M.N., Ibrahim, N.S., 2015. Physico-mechanical, microstructure characteristics and fire resistance of cement pastes containing Al₂O₃ nano-particles. *Construction and Building Materials*, 91, p. 232-242. <https://doi.org/10.1016/j.conbuildmat.2015.05.036>.
- [49] Brazilian Association of Technical Standards - ABNT. ABNT NBR 8082: *Rigid polyurethane foam for heat insulation purposes: Determination of compressive strength.* ABNT. 2016.
- [50] Tabelin, C.B., Veerawattananun, S., Ito, M., Hiroyoshi, N., Igarashi, T., 2017. Pyrite oxidation in the presence of hematite and alumina: I. Batch leaching experiments and kinetic modeling calculations. *Sci. Total Environ.* 580, p. 687-698. <https://doi.org/10.1016/j.scitotenv.2016.12.015>.
- [51] Ram, S., 2001. Infrared spectral study of molecular vibrations in amorphous, nanocrystalline and AlO(OH) αH₂O bulk crystals. *Infrared Phys. Technol.* 42, p. 547-560. [https://doi.org/10.1016/S1350-4495\(01\)00117-7](https://doi.org/10.1016/S1350-4495(01)00117-7).
- [52] Laoutid, F., Bonnaud, L., Alexandre, M., Lopez-Cuesta, J.M., Dubois, P., 2009. New prospects in flame retardant polymer materials: from fundamentals to nanocomposites. *Mater. Sci. Eng. R.*, 63, p. 100-125. <https://doi.org/10.1016/j.mser.2008.09.002>.
- [53] Yang, R., Hu, W., Xu, L., Song, Y., Li, J., 2015. Synthesis, mechanical properties and fire behaviors of rigid polyurethane foam with a reactive flame retardant containing phosphazene and phosphate. *Polym. Degrad. Stabil.* 122, p. 102-109. <http://dx.doi.org/10.1016/j.polymdegradstab.2015.10.007>.
- [54] Singh, H., Jain, A.K., 2008. Ignition, combustion, toxicity, and fire retardancy of polyurethane foams: A comprehensive review. *Journal of Applied Polymer Science*, 111, p. 1115-1143. <https://doi.org/10.1002/app.29131>.
- [55] D'Amore, G.K.O., Caniato, M., Travan, A., Gianluca, T., Marsich, L., Ferluga, A., Schmid, C., 2017. Innovative thermal and acoustic insulation foam from recycled waste glass powder. *J. Clean. Prod.*, 165, p. 1306-1315. <https://doi.org/10.1016/j.jclepro.2017.07.214>.

CONCLUSÃO

Compósitos de PU foram preparados com cimento, areia, GLA e AAS. Este estudo demonstra que estes insumos podem ser usados como matéria-prima para a produção de placas para construção civil.

As placas obtidas apresentaram resistência acústica, térmica e inflamabilidade utilizando 24,5% de resíduos da lapidação de vidro ou da anodização do alumínio que seriam destinados a aterros. Deste modo, resíduos ganharam novo ciclo de vida, evitando extração, foi possível o reaproveitamento de descartes.

Foi verificado através SEM que a substituição de cimento por areia ou pelos resíduos manteve a estrutura alveolar, mas houve uma redução na resistência mecânica das espumas rígidas. Os compósitos desenvolvidos no estudo foram resistentes à propagação horizontal, mas não resistentes a propagação vertical de chama. Os compósitos não apresentaram diferenças significantes de comportamento de barreira sonora até 250 Hz e em 16000 Hz, no entanto agiram como barreira sonora nas frequências de 1000 Hz, 2000 Hz, 4000 Hz e 8000 Hz. PuCemAas e PuCemGla foram mais isolamento térmico que PuCemSan e PuCem.

O compósito com PuCemSan apresentou três resultados superiores que foram inflamabilidade horizontal, acústico e compressão mecânica, seguido do PuCemAas destacando bons resultados nos testes de propagação a chama. Assim o uso de AAS como alternativa tecnicamente viável para reduzir o uso de matérias-primas de fontes não renováveis. Mais pesquisas são recomendadas para atender a essas demandas. As limitações deste estudo

incluem a falta de estimativas de custo e viabilidade econômica para a produção em larga escala de painéis.

Desse modo, o desenvolvimento de produtos buscando soluções, conhecimento e inovação para problemas atuais, poupança do meio ambiente e que tragam qualidade de vida para geração atual e não impactem na geração futura.